

# The Structure of Lipid Bilayers Adsorbed on Activated Carboxy-Terminated Monolayers Investigated by Sum Frequency Generation Spectroscopy

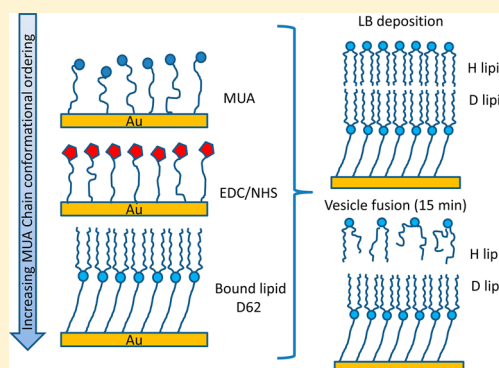
Michael T. L. Casford,<sup>‡</sup> Aimin Ge,<sup>†</sup> Peter J. N. Kett,<sup>‡</sup> Shen Ye,<sup>\*,†</sup> and Paul B. Davies<sup>\*,‡</sup>

<sup>†</sup>Catalysis Research Center, Hokkaido University, Sapporo, 001-0021 Japan

<sup>‡</sup>Department of Chemistry, University of Cambridge, Lensfield Road, Cambridge, CB2 1EW United Kingdom

## S Supporting Information

**ABSTRACT:** The formation and structure of isotopically asymmetric supported bilayer membranes (SBMs) has been investigated using sum frequency generation (SFG) vibrational spectroscopy supplemented by reflection absorption infrared spectroscopy (RAIRS). The bilayers were composed of a proximal and distal leaflet of the phospholipid dipalmitoyl phosphatidylethanolamine (DPPE) supported on a gold surface. The proximal leaflet was chemically tethered to the gold via an 11-mercapto-undecanoic acid (MUA) self-assembled monolayer (SAM) that had been chemically modified to produce an activated succinimide headgroup using *N*-hydroxysuccinimide (NHS) and *N*-(3-dimethylaminopropyl)-*N'*-ethylcarbodiimide (EDC). The activation of the MUA and the tethering of the DPPE were monitored and confirmed using SFG and RAIRS. The distal leaflet of the bilayer was added using either vesicle fusion (VF) or Langmuir–Blodgett (LB) deposition. To gain insight into the structure of each layer of the SBM perdeuterated DPPE (d-DPPE) and MUA (d-MUA) were used to create SBMs with a layer that was isotopically distinguishable from the rest. The polar orientation and conformational ordering of the lipids was determined using SFG. It was found that the tethering of the proximal lipid leaflet resulted in an increase in the conformational order of the MUA SAM. Furthermore, by careful analysis and comparison of spectra recorded in both the C–H (2800–3000 cm<sup>−1</sup>) and C–D (2000–2300 cm<sup>−1</sup>) stretching regions it was concluded that a better ordered and more biologically relevant lipid bilayer was formed when the distal leaflet was added using LB deposition. On the other hand the SFG spectra of the SBMs in which the distal leaflet was added by VF showed little evidence of conformational ordering on the time scale of minutes, suggesting the presence of an incomplete monolayer or of multilayer formation.



## INTRODUCTION

The membrane of a biological cell plays a crucial role in preserving the cell structure, maintaining homeostasis within the cell and facilitating intercell interactions.<sup>1</sup> Biological membranes are complex environments containing a vast array of different phospholipids, proteins, carbohydrates, and sterols. This complexity has made it difficult to identify the role and function of individual components of the membrane, and has led to the development of supported bilayer membranes (SBMs)<sup>1</sup> as model systems to begin to understand the structure, function, and interactions between the different biomolecules.<sup>2</sup> As with any biological system it is important to study such systems *in situ* and if possible immersed in a biologically relevant medium.

Hybrid bilayer membranes (HBMs)<sup>3,4</sup> are a category of SBMs in which a lipid distal leaflet is deposited on a proximal leaflet formed by self-assembly on a solid metal or dielectric substrate. On metal surfaces the proximal leaflet consists of a self-assembled monolayer (SAM) of a long-chain aliphatic thiol covalently bound to the metal substrate by a strong metal–

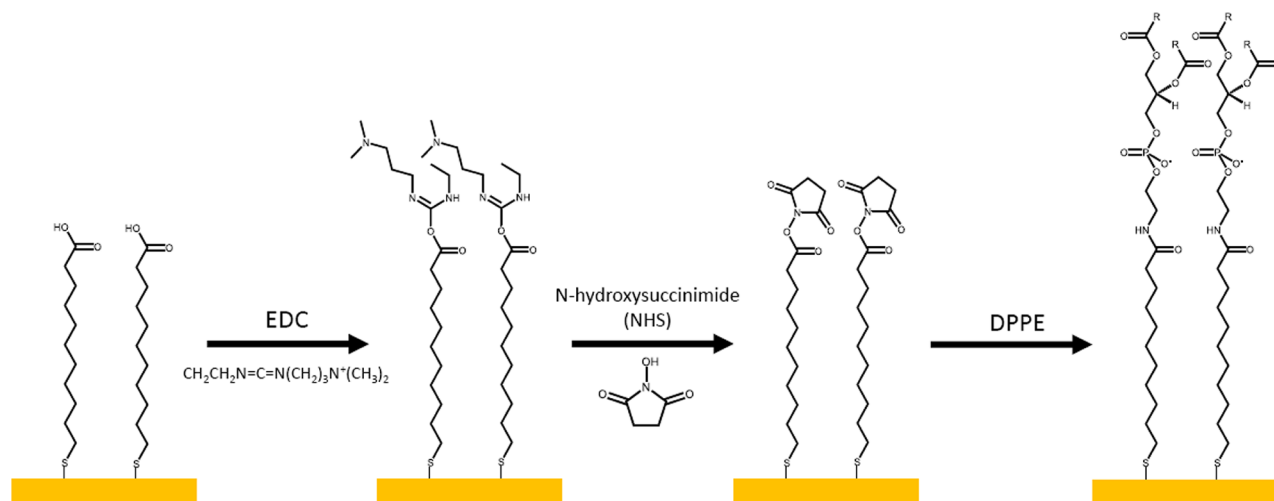
sulfur bond.<sup>5</sup> From a biological perspective a highly condensed aliphatic thiol SAM is a much more rigid structure than the leaflets of a typical lipid membrane. This limitation can be overcome using SBMs in which a hydrophilic anchoring SAM, typically comprising a short-chain carboxylic acid, has been covalently bound to a solid support in order to allow the linking of a lipid monolayer or bilayer via the well established *N*-(3-dimethylaminopropyl)-*N'*-ethylcarbodiimide (EDC)/*N*-hydroxy succinimide (NHS) activation procedure.<sup>6</sup> For example an activated SAM of mercapto-undecanoic acid (MUA) on gold can be covalently linked via an amide bond to a monolayer of the lipid dipalmitoylphosphatidylethanolamine (DPPE). The activation of carboxy-terminated alkyl chains on silicon surfaces has previously been investigated by Touahir et al.<sup>7,8</sup> using linear attenuated total reflection (ATR) infrared spectroscopy which is surface sensitive but not surface specific. They concluded that

Received: October 21, 2013

Revised: March 3, 2014

Published: March 14, 2014

Scheme 1



formation of a succinimide ester on the surface to activate the carboxy group requires careful control of the reaction temperature and the concentration of the reactants in order to prevent unwanted side reactions producing unreactive *N*-acylurea that can block the surface activation sites. The first two reaction steps in Scheme 1 illustrate how the succinimide ester of MUA is formed using the EDC/NHS protocol, and the third step illustrates how the proximal lipid leaflet is bound to the activated SAM by an amide link.

The SBM is completed by one of two common methods. Vesicle fusion (VF)<sup>9</sup> in which the distal lipid leaflet is deposited from vesicles in solution or Langmuir–Blodgett (LB)<sup>10</sup> deposition in which a lipid monolayer is first formed at the air water interface of a Langmuir trough before casting onto the activated solid support. As most commonly used, vesicle fusion onto a hydrophilic surface gives rise directly to an isotopically homogeneous lipid bilayer, which is appropriate when isotopic labeling of the individual lipid leaflets is not required. However if isotopic labeling of one lipid leaflet in a bilayer is required to distinguish it spectroscopically from the other, a proximal monolayer must first be produced by self-assembly onto the activated substrate followed by formation of an isotopically distinguishable distal leaflet by vesicle fusion onto the hydrophobic proximal leaflet. Alternatively, the isotopically distinguishable distal leaflet may be added by LB deposition which has the advantage over VF that the compression of the film can be controlled, enabling different phases of the film to be selected as the distal leaflet.<sup>10</sup> An additional benefit of the LB method is that the time frame for construction of the distal leaflet is in the order of 10 min, thus minimizing any potential isotopic equilibration of the two leaflets due to the lipid flip–flop mechanism in any unbound lipid.

In this study, we directly compare the structures of SBMs in which the distal leaflet is added by either VF or LB deposition. Both techniques are commonly used in the formation of SBMs although there are few examples in the literature of studies that have employed both techniques and directly compared the structures of the SBMs that are formed. An exception is the work of Lipkowski and co-workers who used scanning tunneling microscopy (STM), atomic force microscopy (AFM), and polarization modulation infrared reflection absorption spectroscopy (PMIRRAS) to compare the structures of dimyristoyl phosphatidylcholine (DMPC) bilayers

deposited directly onto planar gold surfaces by either vesicle fusion or LB deposition.<sup>11,12</sup> They imaged the bilayers using AFM and STM and looked at the effect on the structure of the DMPC bilayer of changing the charge on the gold surface. Overall they concluded that more uniform and ordered bilayers were formed using LB deposition. They found that LB deposition resulted in the formation of lipid bilayers in which the alkyl chains were less tilted and in which there was a narrower distribution of tilt angles. Bilayers formed using vesicle fusion were found to be thinner and generally more disordered.<sup>11,12</sup>

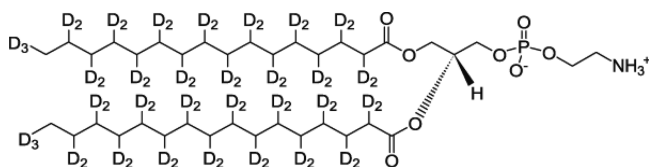
The structure of SBMs formed using LB or VF deposition has been investigated using a number of different spectroscopic and nonspectroscopic techniques. These include AFM<sup>13</sup> and fluorescence microscopy<sup>14</sup> to image the SBM and determine the thickness, uniformity, and fluidity of the bilayer. Quartz crystal microbalance (QCM)<sup>15</sup> and surface plasmon resonance (SPR)<sup>16</sup> methods have been used to investigate the mechanism and kinetics of bilayer formation, and reflection absorption infrared spectroscopy (RAIRS),<sup>4</sup> surface enhanced Raman spectroscopy (SERS),<sup>5</sup> and attenuated total reflectance spectroscopy (ATR)<sup>17</sup> to obtain structural information on the orientation and conformational ordering of the lipid molecules.

In this investigation the structure of the activated MUA SAM and of monolayers and bilayers formed on it by VF or LB deposition has been investigated using sum frequency generation (SFG)<sup>18–20</sup> vibrational spectroscopy, a nonlinear optical technique that is interface specific, supplemented by reflection absorption infrared spectroscopy (RAIRS). In the SFG technique two pulsed laser beams, one at a fixed visible frequency and the other a tunable infrared laser, are combined temporally and spatially on a surface or interface. As a result of the breakdown of symmetry at the interface SFG light is emitted at the sum of the two input frequencies. A vibrational spectrum of the interfacial molecules is recorded by measuring the change in the SFG beam intensity as the infrared laser frequency is tuned. Alternatively a broad band infrared source may be used. SFG spectroscopy determines, subject to certain selection rules, the polar orientation and conformational ordering of the functional groups in the membrane. For example, in the C–H stretching region aliphatic chains can potentially give rise to spectra from methyl (r resonances) or methylene groups (d resonances). When spectra are recorded

on metal surfaces there is both a frequency-independent nonresonant contribution to the signal from the metal surface and a resonant contribution to the signal from the lipid film. Interference between these signals yields information on the polar orientation of the adsorbed molecules. By using per-protonated and per-deuterated versions of each layer, it is then possible to use SFG spectroscopy to determine the structure of the individual layers occurring in the multilayer film. In this article we obtain and interpret the SFG spectra of each layer as it is added to make up the SBM film and the effect of the added layer on the structure of the underlying layer or layers.

## EXPERIMENTAL SECTION

**Materials.** Per-protonated mercapto-undecanoic acid (MUA) (Sigma Aldrich 98%), per-deuterated mercapto-undecanoic acid (d-MUA) (CK gas products), *N*-(3-dimethylaminopropyl)-*N*'-ethylcarbodiimide (EDC) and *N*-hydroxy succinimide (NHS) (Sigma Aldrich), 1,2 dipalmitoyl *sn* glycerol-3-phosphoethanolamine (h-DPPE) and per-deuterated 1,2 dipalmitoyl D62 *sn* glycerol-3-phosphoethanolamine (d-DPPE) shown below (Avanti polar lipids) were used as received.



**Formation of the Bound SBM.** MUA samples were prepared in methanolic solution in micromolar concentrations. Generally  $\sim 0.001$  g of thiol was added to  $\sim 5$  mL of methanol. The MUA was left to self-assemble on gold-coated substrates at room temperature for a minimum of 24 h. Prior to self-assembly the gold substrates were UV ozone cleaned for 30 min. RAIRS spectra of both MUA and d-MUA coated substrates confirmed the presence of a surface carboxylate. After the SAM formation was complete, samples were removed from the methanolic solution, rinsed in Millipore water ( $18.2 \text{ M}\Omega \text{ cm}^{-1}$ ) and activated by placing them in 5 mM EDC/NHS aqueous solutions for 2 h at  $5^\circ \text{C}$  following the procedure of Touahir et al.<sup>7,8</sup> Immediately following activation the samples were rinsed in Millipore water and dried under a nitrogen stream before being placed in DPPE dissolved in 1 mg/mL chloroform (HPLC grade) overnight and finally rinsed in chloroform and dried. The distal DPPE envelope, per-protonated or per-deuterated, was then formed either by immersion in lipid vesicle buffer solution followed by rinsing in Millipore water or by LB deposition. Samples were kept immersed under Millipore water in a sealed sample cell, and all spectra were recorded under water. At no stage was the lipid bilayer exposed to air.

**Preparation of DPPE Vesicles.** One milligram of DPPE was sonicated in 1 mL of tris buffer at  $65^\circ \text{C}$ . The extruder was heated to  $65^\circ \text{C}$  on a heating block and the solution extruded 10 times, until the final solution appeared clear. Vesicle solution was injected into the sample cell in which a DPPE monolayer covalently bound onto MUA had previously been mounted. The sample was left immersed for a selected immersion time and flushed with Millipore water, and the cell was finally sealed.

**LB Deposition.** DPPE (1 mg/mL) was dissolved in chloroform and 30  $\mu\text{L}$  cast onto the surface of an LB trough (NIMA 311 or FSD-500, USI System) using a microliter

syringe. The chloroform was allowed to evaporate and the surface compressed to give an interfacial tension of  $40 \text{ mN m}^{-1}$ . The sample, held horizontally, was then lowered through the interface into a sample cell filled with Millipore water, and the cell was sealed.<sup>21</sup>

**SFG Spectroscopy.** A complete theoretical description of SFG can be found elsewhere,<sup>18–20</sup> and only a brief summary is given here. Due to the metal surface selection rule and the high reflectivity of metal surfaces in the IR region only polarization combinations that contain *p*-polarized IR light give rise to significant SFG intensity on a metal surface. Therefore, for the gold substrates used throughout this work, only the SSP (corresponding to *s*-polarized SFG, *s*-polarized visible, and *p*-polarized IR) and PPP polarization combinations are suitable. In the SSP polarization combination only a single component of the nonlinear susceptibility tensor, namely  $\chi^{(2)}_{xxxz}$  is probed; hence, only vibrational modes having transition dipole moments perpendicular to the surface are SFG active. On the other hand, spectra in the PPP combination contain contributions from several susceptibility components, specifically  $\chi^{(2)}_{zzzz}$ ,  $\chi^{(2)}_{xxzz}$ ,  $\chi^{(2)}_{zzxx}$  and  $\chi^{(2)}_{xxxx}$ . IR active vibrations in both the *z* and *x* axes are therefore potential sources of SFG signals in the PPP beam polarization; i.e., this polarization probes vibrational resonances with transition dipoles oriented both parallel and perpendicular to the surface. Furthermore the SSP spectra are usually at least an order of magnitude weaker than those in the PPP polarization due to the near cancellation of the incident and reflected fields of the IR laser due to the high reflectivity of gold in the IR region and the dominance of the  $\chi^{(2)}_{zzz}$  term from the gold surface which only occurs for the PPP polarization. For a vibrational mode to be SFG active it must be simultaneously infrared and Raman active. Hence, any functional group that has a localized center of symmetry will be SFG inactive by the rule of mutual exclusion. As a consequence in a long all-trans-hydrocarbon chain the methylene groups will be SFG inactive, and no methylene (d resonances) will be observed. Conversely the presence of d resonances in the spectrum leads to the conclusion that there are gauche defects in the chain.<sup>19</sup>

The SFG spectra were modeled using a least-squares Levenberg–Marquardt algorithm<sup>22</sup> that fitted the resonances to Lorentzian line profiles derived from the SFG equation. The modeling allowed for the frequency, integrated intensity, and widths of the vibrational resonances to be determined, as well as the intensity and phase of the nonresonant susceptibilities. As the phase term for the adsorbate is purely imaginary, it is constrained to be either  $\pm 90^\circ$ , depending on the orientation of the molecule. The phase of the metal surface can take any value but can be considered constant for any given metal/adsorbate combination. In the case of a thiol bound onto gold the phase of the gold surface is well established and is usually quoted at  $\sim 90^\circ$ . This gives rise to the resonances appearing as either positive or negative going bands with a Lorentzian profile. The relative phases for fitting the  $d^+$  and  $d^+_{\text{FR}}$  signals have been constrained in the modeling to a single value on grounds of symmetry. Further details of the fitting can be found in the Supporting Information (SI).

Sum frequency generation spectroscopy was carried out using both a broadband femtosecond SFG spectrometer based on a Ti-sapphire laser (Spectra-Physics) and OPO (TOPAS, Light Conversion)<sup>23</sup> and a narrowband picosecond Nd:YAG laser (Ekspla PL4431B) and OPO (Ekspla PG401) SFG spectrometer,<sup>24</sup> both operating in a copropagating beam



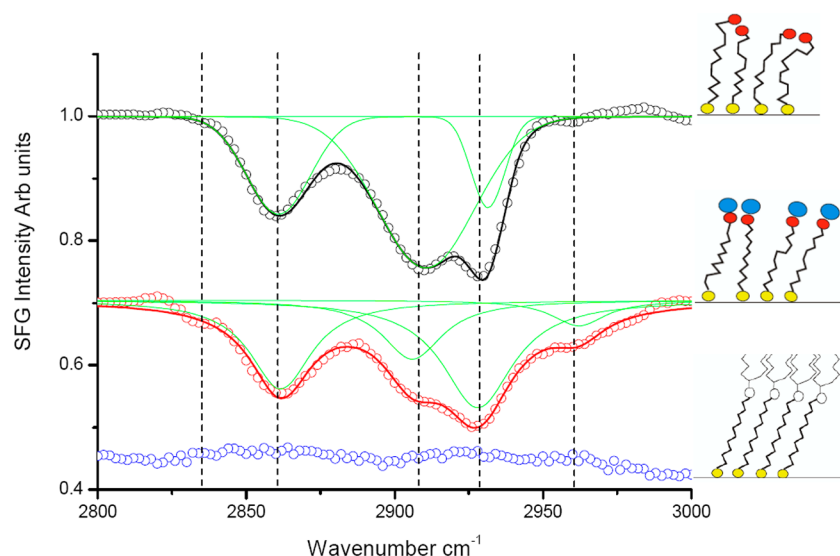


**Figure 1.** SFG spectra of a MUA SAM on gold in the PPP polarization combination and in the C–H stretching region. In this and later figures experimental data points are indicated by open circles, fits to the data by solid lines, deconvoluted fitted resonances by green lines and fitted line positions (given in the text) by vertical dashed lines. Top spectrum in black, before activation; middle spectrum in red, after EDC/NHS activation; bottom spectrum in blue, with a d-DPPE film on top of the activated MUA SAM.

geometry with angles of incidence of  $60^\circ$  and  $55^\circ$  for the visible and IR beams, respectively. The fast acquisition time of the femtosecond spectrometer complemented the higher spectral resolution of the picosecond system and allowed the rapid accumulation of multiple repeats ensuring the reproducibility of the results. The increased resolution of the picosecond spectrometer reduced the uncertainty inherent in the spectral modeling which was required to accurately assign the resonances of the MUA monolayer. Unless stated otherwise the spectra presented in the figures were recorded with the picosecond spectrometer. Representative spectra showing the relative resolution of picosecond and femtosecond spectra of the same MUA film are presented in the SI, Spectrum S1a.

**RAIRS and Linear IR Spectroscopy.** Linear IR and RAIRS spectra were recorded on a Perkin-Elmer FTIR 100 spectrometer fitted with a liquid nitrogen cooled mercury cadmium telluride (MCT) detector. In general 256 scans were coadded to give the final spectrum with a minimum of three repeats carried out on different samples. RAIRS spectra were recorded on a Specac grazing angle accessory set at an angle of incidence of  $70^\circ$ . Bulk IR spectra of solvent cast thick films were recorded on a Perkin-Elmer 7 reflection horizontal ATR accessory using a germanium top plate and corrected for penetration depth using the ATR correction algorithm provided in the Spectrum 6 software.

## RESULTS AND DISCUSSION

**Spectra of MUA SAMs on gold.** We first describe and interpret the SFG spectra of MUA and d-MUA SAMS under air, and their complementary RAIRS spectra. The SFG spectra of a SAM of MUA on gold under air in the PPP polarization combination and in the C–H stretching region are shown in Figure 1. (The corresponding SSP polarization spectrum is shown in SI, Spectrum S1b.)

The MUA spectrum (top) comprises three distinct spectral dips with their centers modeled at 2860, 2908, and 2932  $\text{cm}^{-1}$ . The positions of these resonances are very similar to those observed by Asanuma et al.<sup>25</sup> in the SFG spectra of alkoxy-terminated dodecyl monolayers on silicon and assigned by

them to methylene stretching modes, namely the  $d^+$  symmetric stretch, the  $d^-_{\omega}$  stretch, (the asymmetric stretch of the methylene group adjacent to the carboxylic acid headgroup), and the  $d^-$  asymmetric stretch, respectively. However, they regarded as tentative<sup>25</sup> the assignment of the 2908  $\text{cm}^{-1}$  resonance to the  $d^-_{\omega}$  mode. The fact that all three  $d$  resonances in the spectrum appear as dips indicates that the SFG resonant signals of the methylene groups destructively interfere with the nonresonant SFG signal of the gold substrate. For the monolayer film considered here in the copropagating geometry, signal dips have been shown to correlate with a net polar orientation of the adsorbed monolayer methylene groups away from the substrate surface. Spectra of d-MUA SAMS recorded in the C–D region at  $\sim 2100 \text{ cm}^{-1}$  were weaker and exhibited only two resonances. A d-MUA spectrum in the PPP polarization combination is shown in the SI, Spectrum S2.

An alternative assignment of the two resonances Asanuma et al. assigned as  $d^-$  is suggested by employing polarization spectroscopy analysis as developed by Lu and co-workers<sup>26</sup> for assigning methylene resonances. Their analysis showed that, at the liquid/air interface, resonances from symmetric methylene stretching modes should be many times stronger in SSP polarization spectra than in PPP polarization spectra. Conversely resonances of asymmetric methylene modes should be stronger in the PPP than the SSP polarization. The SSP spectrum of a MUA melt ( $\sim 320 \text{ K}$ ) in air (SI, Spectrum S3) is very similar to the three principle resonances in both PPP and SSP polarizations of a MUA SAM on gold (Figure 1 and spectrum S1b SI). Furthermore these three resonances are essentially absent in the PPP spectrum of the melt implying that all three must arise from symmetric methylene stretching modes. It is therefore most likely that, as suggested by Lu et al.,<sup>26</sup> these resonances are indeed all due to the  $d^+$  symmetric stretch and its associated Fermi resonances. The positions of the resonances are 2849, 2908, and 2932  $\text{cm}^{-1}$ . With the exception of the lowest frequency resonance the positions of the other two resonances are in excellent agreement with their positions in the spectrum of the MUA SAM. The shift in the position of the lowest frequency resonance between the

position in the melt, which corresponds to the  $d^+$  frequency of Asanuma et al., and its frequency in the SAM is interesting. Two possible explanations are either because the position of the  $d^+$  resonance is particularly susceptible to surface effects such as the electron-withdrawing effect of the strong gold thiol bond or because the conformational order of the MUA monolayer is different from that observed in the melt, thus leading to differing intensities in the  $CH_2$  contribution from the chain body and the terminal  $CH_2$  groups.

SFG spectra of MUA SAMs were also recorded in the C–O stretching region. The only resonances detected between 1400  $cm^{-1}$  and 1800  $cm^{-1}$  are shown in Figure 2. The more intense

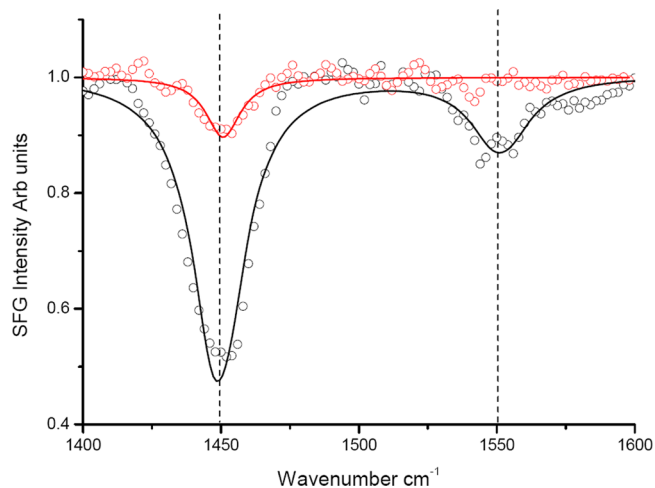


**Figure 2.** SFG spectrum of a MUA SAM on gold in the carboxylate stretching region. PPP spectrum in black, SSP spectrum magnified 6-fold in red.

PPP polarization spectrum comprises two resonances with frequencies modeled at 1449 and 1551  $cm^{-1}$  corresponding to the symmetric and asymmetric carboxylate C–O stretching vibrations, respectively. In the SSP polarization only the symmetric stretching mode appears in the spectrum, but this may be due to the much lower experimental signal-to-noise ratio in this polarization combination.

The corresponding RAIRS spectrum of a MUA SAM in the C–H stretching region is shown in Figure 3 (lowest spectrum). There are two intense bands at 2851 and 2923  $cm^{-1}$  that can be assigned to the methylene  $d^+$  and  $d^-$  stretching modes of MUA, respectively, by comparison with the IR transmission spectrum (not shown). Interestingly the position of the  $d^+$  band corresponds closely to its position in the SFG SSP spectrum at the liquid/air interface while the  $d^-$  band is absent in the corresponding PPP spectrum, presumably due to poor overlap between the IR and Raman band positions. There is a further contribution to the RAIRS spectrum from a weaker, broad band centered at  $\sim 2900$   $cm^{-1}$  present as a shoulder on the  $d^-$  band that can be assigned to the  $d^+_{FR}$  mode. This is also a candidate for one of the two  $d$  resonances in the SFG spectra tentatively assigned as  $d^+$ . It is reasonable to conclude that the high intensity of the  $d^+$  and  $d^-$  bands in the RAIRS spectrum means that they must arise from the relatively large number of methylene groups in the aliphatic chain. Conversely, the bands from the methylene group adjacent to the carboxylate end group, presumably at different frequencies, are too weak to observe in the RAIRS spectrum.

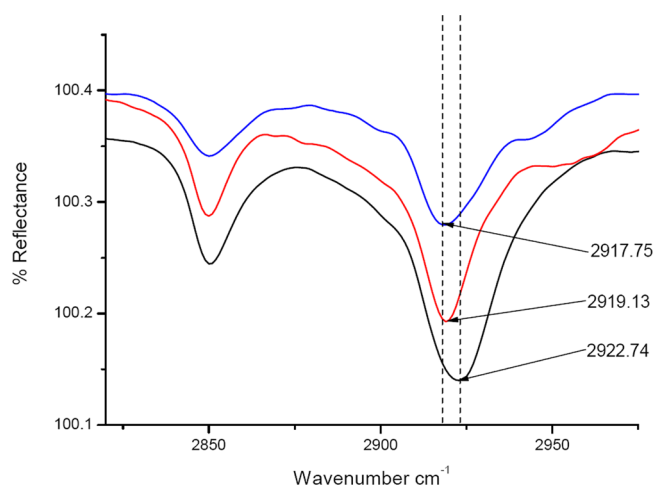


**Figure 3.** RAIRS spectra in the C–H stretching region of a MUA SAM on gold (bottom spectrum), a NHS/EDC activated SAM on gold (middle spectrum), and a d-DPPE monolayer on an activated SAM on gold (top spectrum).

The position of the asymmetric methylene stretching band is sensitive to conformational ordering and can be used as a qualitative measure of the ordering of the aliphatic chain in a molecule. As an alkyl chain becomes more ordered, the  $d^-$  band shifts to lower frequencies. For an ODT SAM on gold where the alkyl chains have a high degree of conformational order and contain few gauche defects, the  $d^-$  band in the RAIRS spectrum lies at 2916  $cm^{-1}$ . Generally a frequency of 2918  $cm^{-1}$  is used as a qualitative indication of the change from a disordered to an ordered alkyl chain. The position of the  $d^-$  band of an MUA SAM before activation, 2923  $cm^{-1}$  (lowest spectrum Figure 3) is therefore indicative of an alkyl chain containing a significant population of gauche defects. The same conclusion on the conformational ordering of the MUA chain in the SAM prior to activation was reached above from the presence of  $d$  resonances in the SFG spectrum. It seems therefore that the hydrocarbon chains of an MUA SAM are more disordered than those in an ODT SAM on gold. This is reasonable given both the shorter chain length and the bulkier acid headgroup of MUA impairing close packing of the alkyl chains.

The RAIRS spectrum of a d-MUA SAM on gold between 1300 and 2300  $cm^{-1}$  is shown in Figure 4 (black spectral line). The bands at 2096 and 2198  $cm^{-1}$  arise from the C–D  $d^+$  and  $d^-$  modes of the methylene groups and are analogous to the C–H bands shown in Figure 3. The bands at 1451 and 1545  $cm^{-1}$  arise from the carboxylate symmetric and asymmetric C–O stretching modes, respectively, corresponding to the SFG resonances shown in Figure 2. There is no evidence of the carboxylic acid C=O stretching band, expected to lie at  $\sim 1750$   $cm^{-1}$ , in the RAIRS and SFG spectra of either MUA or d-MUA SAMs, implying that the terminal carboxylic acid groups in the SAM may be fully ionized.

**Spectra of Activated MUA SAMs on Gold.** The SFG spectrum of an EDC/NHS activated MUA SAM in the C–H stretching region is shown in the middle trace in Figure 1 and is clearly analogous to the spectrum prior to activation. Three spectral dips can be modeled at the same frequencies, namely 2860, 2908, and 2932  $cm^{-1}$ . However, the resonance at 2908  $cm^{-1}$  now has significantly lower intensity relative to that of the other resonances. This suggests that its orientation is particularly susceptible to the change of structure accompany-

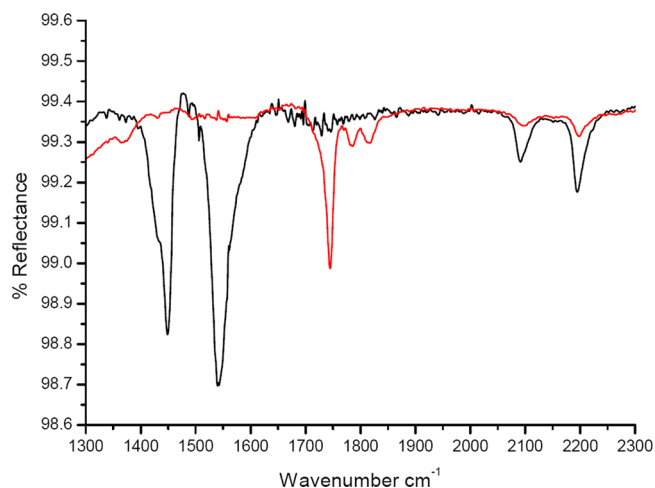


**Figure 4.** RAIRS spectra of d-MUA (black) and activated d-MUA (red) SAMs.

ing activation, supporting the assignment of this resonance to the methylene group adjacent to the carboxylic acid group. Additionally a new spectral dip, modeled at  $2956\text{ cm}^{-1}$ , appears as a shoulder on the  $2932\text{ cm}^{-1}$  resonance. This resonance could be assigned to the C–H symmetric stretching mode ( $d^+$ ) of the methylene groups of the succinimide ring of the ester which is both infrared ( $2945\text{ cm}^{-1}$ , in  $\text{CDCl}_3$ )<sup>27</sup> and Raman ( $2960\text{ cm}^{-1}$ , solid)<sup>28</sup> active in succinimide. However, it is more likely that it originates from the MUA itself for which a band at  $2950\text{ cm}^{-1}$  is present at the liquid/air interface (from the melt, Spectrum S3 [SI]). Significantly no band can be modeled at  $2956\text{ cm}^{-1}$  in the SFG spectrum of an activated d-MUA SAM (Figure 6). The SFG spectra recorded in the C–O stretching region following activation of MUA or d-MUA SAMs contained no detectable resonances in either polarization, i.e. the carboxylate resonances shown in Figure 2 disappeared on activation (spectrum not shown).

The corresponding RAIRS spectra of the C–H and C–D stretching bands of MUA (Figure 3) and d-MUA (Figure 4) on activation show a decrease in intensity. This can be attributed to the alkyl chains of MUA adopting an orientation such that the plane of the  $\text{CH}_2$  groups lies closer to the plane of the metal surface following activation. The change in the RAIRS spectra in the C–H (C–D) regions on activation is compatible with the decrease in the intensity of the middle resonance in the PPP SFG spectrum (Figure 1). An analogous decrease in the SFG and RAIRS spectra of a MUA SAM, attributed to greater conformational order, has been reported previously in a study of electrostatic layer-by-layer assembly of PEI/PAZO polyelectrolytes on MUA SAMs.<sup>29</sup> Furthermore, the shift in the position of the  $d^-$  band on activation to  $2919\text{ cm}^{-1}$  (Figure 3) confirms that the conformational order increases on activation. This would permit closer packing of the chains. Interestingly the RAIRS spectrum of the activated MUA SAM now has a weak band at  $\sim 2960\text{ cm}^{-1}$  which is absent before activation and is at a frequency similar to that of the resonance that appears in the SFG spectrum of the activated MUA at  $2956\text{ cm}^{-1}$  mentioned above.

The disappearance of the carboxylate bands in the SFG spectrum on activation is also observed in the RAIRS spectrum of d-MUA (Figure 4, red trace) and MUA (not shown). Furthermore three bands associated with the formation of a succinimidyl ester (Scheme 1) appear in the RAIRS spectrum

of activated d-MUA (Figure 4) and activated MUA, namely the C=O stretching modes of the succinimidyl ring ( $1745$  and  $1789\text{ cm}^{-1}$  respectively) and the C=O mode of the ester group ( $1825\text{ cm}^{-1}$ ).<sup>8</sup> Lastly the main vibrational band characteristic of *N*-acyl urea formation lies at  $1650\text{ cm}^{-1}$  and this was not observed in either the SFG or RAIRS spectra i.e. there is little evidence for the presence of this molecule in the monolayer.

The overall conclusion that can be drawn from the changes to the SFG and RAIRS spectra that occur on activation is that a succinimidyl ester-terminated MUA monolayer has been formed that exhibits an increased conformational ordering in comparison to the unactivated MUA SAM (Scheme 1).

**Spectra of DPPE Monolayers Deposited on Activated MUA SAMs.** The next step in the formation of the supported bilayer membrane was to adsorb a proximal lipid layer to the activated MUA monolayer. Figure 5 shows the SFG spectra in the PPP polarization combination recorded in the C–D stretching region from an activated MUA SAM (top) and from a d-DPPE proximal monolayer self-assembled onto an activated MUA SAM from chloroform (middle) and one formed by LB deposition on an activated MUA SAM (bottom). The activated MUA SAM on its own has no obvious resonances in the C–D region, whereas five distinct dips can be modeled for the C–D stretching modes of the d-DPPE monolayers after assembly on the MUA SAM. These lie at  $2070$ ,  $2103$ ,  $2138$ ,  $2187$ , and  $2222\text{ cm}^{-1}$  and are assigned respectively to the  $r^+$ ,  $d^+$ ,  $r^+_{\text{FR}}$ ,  $d^-$ , and  $r^-$  resonances of d-DPPE based on the infrared and Raman spectra reported for deuterated phosphocholines (DPPC)<sup>30</sup> and deuterated stearic acid.<sup>31</sup> The spectra from the self-assembled and LB deposited monolayers are similar with a marginal increase in the  $r^+ : d^+$  amplitude ratio in the LB monolayer.

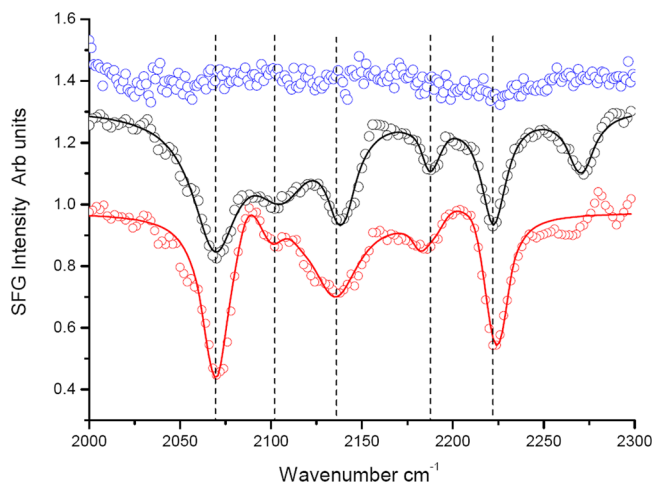


**Figure 5.** SFG spectra in the C–D stretching region and the PPP polarization combination of an activated MUA SAM (blue), a d-DPPE layer formed by self-assembly on an activated MUA SAM (black), and a d-DPPE layer formed by LB deposition on an activated MUA SAM (red).

Although the  $r$  resonances of the d-DPPE monolayer have the highest intensity, the presence of  $d$  resonances indicates that the lipid chains of the bound monolayer contain gauche defects. The phases of the observed methyl and methylene C–D resonances in Figure 5 are the same as for the resonances in the MUA SAM (Figure 1), showing that the monolayer DPPE



molecules are orientated away from the surface, i.e. methyl group uppermost. This is the expected polar orientation since the polar DPPE headgroup displaces the succinimidyl ring on the activated surface to form a new amide link with the MUA SAM (Scheme 1).

The SFG spectrum in the C–H region that accompanies that in the C–D region for self-assembly of the proximal layer shown in Figure 5 is presented in Figure 1. This enables us to determine how adsorption of the d-DPPE monolayer changes the structure of the underlying activated MUA SAM. Prior to adsorption of DPPE the MUA spectrum consists of the three d resonances. Although Asanuma et al.'s assignment of two of the d<sup>+</sup> resonances may be called into question, the absence or reduced intensity of the three d resonances when lipid monolayers are added to the MUA SAM leads to an unambiguous conclusion about the structure of the MUA layer. Due to the symmetry requirement inherent in the SFG selection rules the locally centrosymmetric environment in an all-trans aliphatic chain, i.e. conformationally well ordered with no gauche defects, would render the methylene groups in the chain sum frequency inactive as in the SFG spectrum of an ODT SAM. Furthermore, if one of the d resonances arises from methylene groups at the ends of the chains in positions which are inherently noncentrosymmetric, any reduction in their intensity implies that the molecular dipole must be oriented close to the plane of the metal surface, therefore experiencing a negligible EM field due to the metal surface selection rule. The absence of the d resonances after adsorption of the d-DPPE monolayer shows that (a) the methylene groups in the MUA chains have become conformationally well ordered, i.e. lost their gauche defects, and (b) the dipole of the methylene groups at the ends of the chains have become oriented parallel to the surface. An increase in the conformational order of the chains of an MUA SAM following the adsorption of an overlayer has already been mentioned above.

Turning now to the RAIRS spectra after adsorption of the d-DPPE layer. The RAIRS spectrum still shows the MUA methylene C–H stretching bands (Figure 3) confirming that the MUA SAM remains in place. (A RAIRS survey spectrum of d-DPPE on MUA and DPPE on d-MUA is shown in SI, Spectrum S4.) However, there is a 5 cm<sup>−1</sup> red shift in the position of the asymmetric stretching band after adsorption of the d-DPPE layer which, as noted earlier, corresponds to an increase of conformational order in the MUA SAM. This conclusion is highly compatible with that deduced from the changes in the SFG spectra. Furthermore, there is a substantial drop in RAIRS intensity between an MUA SAM on its own and an activated MUA SAM with an adsorbed layer of d-DPPE, indicating that the dipole moments of the alkyl chain methylene groups are aligned increasingly in the plane of the interface. These changes in the SFG and RAIRS spectra can be accounted for by an increase in conformational ordering of the MUA chains. This may have come about by the reduction in steric hindrance of the MUA headgroup on activation or close packing induced by the chains of the d-DPPE film or both.

To provide support for the above conclusions the spectra of the isotopically complementary combinations of lipid and SAM were examined. The SFG spectra from a DPPE monolayer on an activated d-MUA SAM in the C–H region, the analogue of the d-DPPE/activated MUA spectrum in the C–D region shown in Figure 5, is shown in Figure 6, and its spectrum in the C–D region, in Figure 7. The spectra in both figures confirm the conclusions reached above from considering the

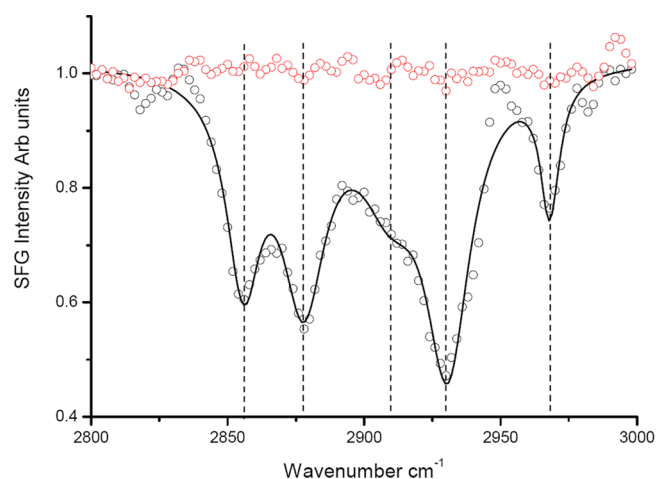


**Figure 6.** SFG spectra in the C–H stretching region and PPP polarization combination of an activated d-MUA SAM (red) and when a DPPE layer is adsorbed on an activated d-MUA SAM (black).

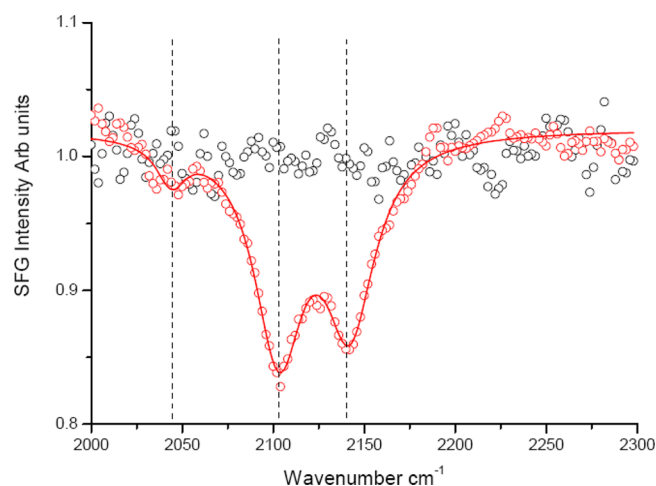


**Figure 7.** SFG spectra in the C–D stretching region and PPP polarization combination of an activated d-MUA SAM (red) and when a DPPE layer is adsorbed on an activated d-MUA SAM (black).

spectra in Figures 1 and 5. First, that although the DPPE molecules in the adsorbed monolayer contain a significant number of gauche defects, the more prominent r resonances show that the monolayer is quite well ordered, but less so than for the same lipid adsorbed on an ODT SAM on gold. Second, adsorption of the DPPE monolayer causes the hydrocarbon chains in the MUA SAM to become conformationally well ordered, i.e. methylene groups all-trans, losing their gauche defects in the process.

Ideally, evidence for the formation of an amide bond would be confirmed by observing a peak in the RAIRS spectrum at 1690 cm<sup>−1</sup>. No such band was observed in the recorded spectra. This has been attributed to the amide C=O bond orienting parallel to the metal surface and therefore being inactive in both RAIRS and SFG due to the metal surface selection rule. In order to confirm the conclusion of the spectroscopic results, namely that the self-assembled monolayer of the lipid has indeed bonded to the activated MUA SAM, the sample was therefore rinsed in two aliquots of chloroform (CHCl<sub>3</sub>). The SFG PPP spectrum in the C–D region recorded immediately after rinsing in CHCl<sub>3</sub> is shown in Figure 8 (upper spectrum). In comparison to the spectrum in Figure 5 the d<sup>+</sup> resonance at

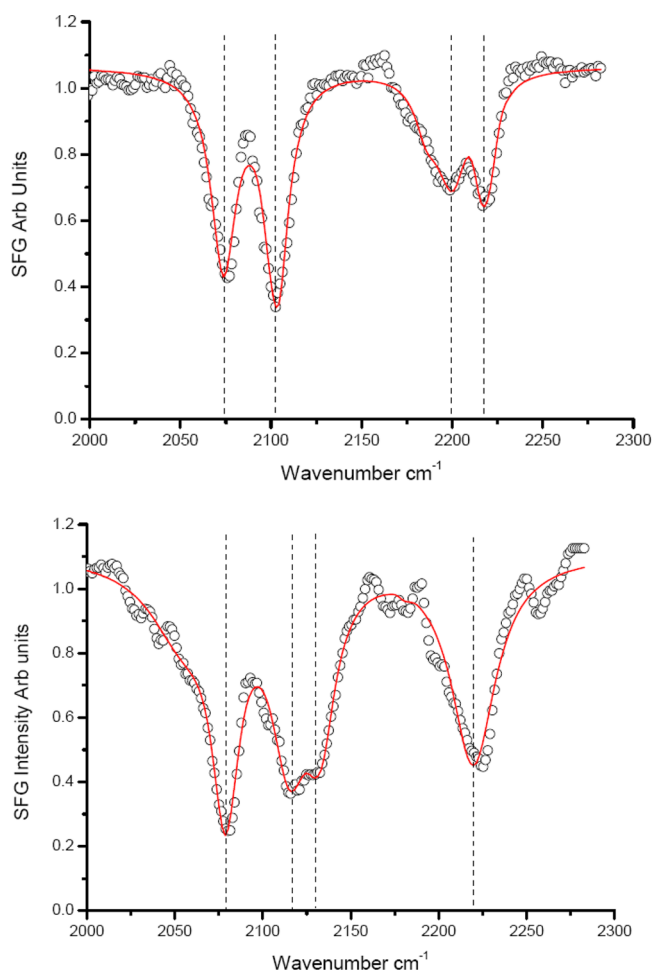


**Figure 8.** SFG spectra in the C–D stretching region and PPP polarization combination of a d-DPPE monolayer self-assembled on an activated MUA SAM after rinsing in  $\text{CHCl}_3$  (upper spectrum) or SDS (lower spectrum).

$2102\text{ cm}^{-1}$  and the  $\text{d}^-$  resonance at  $2182\text{ cm}^{-1}$  are blue shifted and have become significantly stronger, while the  $\text{r}^+_{\text{FR}}$  resonance at  $2131\text{ cm}^{-1}$  has effectively disappeared. These changes indicate an increase in conformational disorder in the lipid chain immediately after rinsing with chloroform. Nevertheless, the strength of the spectra shows that rinsing does not remove the lipid from the surface. Subsequent recordings of the spectrum at longer times after rinsing ( $\sim 1\text{ h}$ ) showed a decrease in the d resonances and an increase in the r resonances so that the spectrum eventually resembled that shown in Figure 5. The presence of a disordered monolayer observed immediately after rinsing slowly returning to a more ordered layer with time can be explained by the gradual evaporation of  $\text{CHCl}_3$  initially incorporated in the film.

The lower spectrum in Figure 8 shows the effect on the DPPE monolayer spectrum after immersion in sodium dodecyl sulfate (SDS) solution for 1 h followed by rinsing with Millipore water. The C–D spectrum is now predominantly due to the methyl r resonances,  $\text{r}^+$  at  $2075\text{ cm}^{-1}$ ,  $\text{r}^+_{\text{FR}}$  modeled at  $2120$  and  $2131\text{ cm}^{-1}$ , and  $\text{r}^-$  at  $2222\text{ cm}^{-1}$ . Modeling the spectrum shows that there is only a small contribution from the methylene d resonances at  $2102$  and  $2184\text{ cm}^{-1}$ . This result, together with the prominence of the methyl resonances, shows that a well-ordered monolayer is present. SDS is routinely used to clean lipid bilayers from QCM quartz crystals and has

previously been shown to remove lipid bilayers physisorbed onto bovine serum albumin (BSA) under the conditions used here.<sup>32</sup> It can therefore be concluded that neither  $\text{CHCl}_3$  nor SDS has the capacity to remove the lipid monolayer from the surface, suggesting that it is chemically (i.e., via an amide bond) rather than physically adsorbed to the activated MUA monolayer. Additionally, the phase of the spectrum recorded under water shows that the hydrophobic alkyl chains rather than the hydrophilic headgroup are oriented into the water phase. Such an orientation is energetically unfavorable and confirms, as expected, that the monolayer has formed an amide bond to the underlying MUA SAM that is strong enough to prevent the monolayer adopting the energetically more favorable reverse orientation when it is immersed in water.

**Bilayer of d-DPPE and DPPE on Activated MUA Formed by Vesicle Fusion.** Finally, after the structures of the lower layers have been determined, the structure of the composite bilayer/substrate film can be investigated. Figure 9

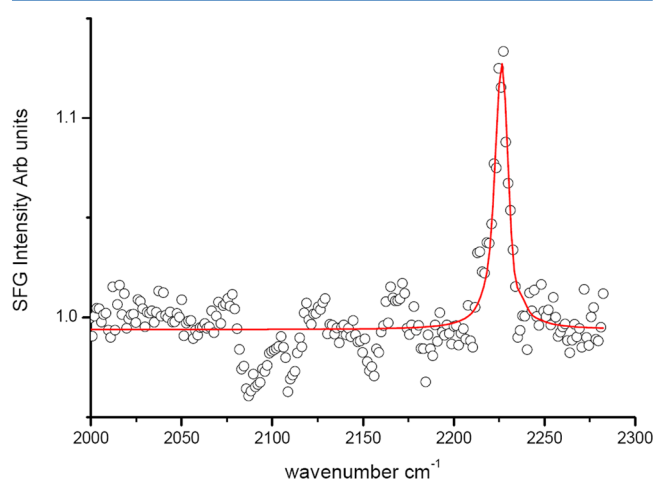


**Figure 9.** SFG spectrum in the C–D stretching region and PPP polarization combination of a bilayer formed by vesicle fusion of d-DPPE on DPPE/activated MUA under water. Spectrum recorded 15 min after introducing the vesicle solution into the sample cell.

shows the SFG PPP spectrum in the C–D region, recorded under water, when a d-DPPE distal leaflet is added by vesicle fusion to a DPPE proximal leaflet formed on an activated MUA SAM. The complex, low-intensity spectrum can only be modeled with a set of overlapping positive and negative resonances and shows only limited evidence of the resonances expected in the C–D region from a deuterated distal monolayer. The only well-defined feature lies at  $2225\text{ cm}^{-1}$  and is tentatively assigned to a C–D  $\text{r}^-$  resonance. The weak C–D spectrum could in principle be due to transfer and incorporation of some d-DPPE molecules into the DPPE proximal leaflet of the bilayer, hence, partially canceling the signal from the distal leaflet. However, the protonated proximal leaflet has been shown above to be essentially close packed and robustly bound to the surface. This suggests that there are few vacant sites for per-deuterated lipid molecules to migrate into the proximal leaflet. A more likely explanation is that over the 15-min time frame of the experiment an incomplete layer of d-DPPE vesicles has adhered to the surface, producing only a partial monolayer on vesicle rupture, leading to the formation of a highly disordered distal leaflet. This conclusion is supported by the spectra of the DPPE leaflet recorded after 3



h which shows significantly better conformational ordering of the distal layer (SI, Spectrum S5).

**Bilayer of d-DPPE and DPPE on Activated MUA Formed by LB Deposition.** In order to compare the quality of the bilayers produced using the LB deposition method with that formed by vesicle fusion an isotopically asymmetric bilayer of DPPE and d-DPPE was formed using LB deposition, with the distal d-DPPE leaflet cast from the surface of a LB trough. The PPP SFG spectrum of the resulting lipid bilayer under water and in the C–D region is presented in Figure 10 (top spectrum).

The signal intensity in this spectrum is much higher than in the corresponding spectrum of the distal layer formed by vesicle fusion (Figure 9). The spectrum is dominated by three strong resonances from the methyl modes of the deuterated distal leaflet of the bilayer with frequencies of 2065 ( $r^+$ ), 2115 ( $r^+_{FR}$ ), and 2216 ( $r^-$ ). One much weaker resonance is also present at  $\sim 2160\text{ cm}^{-1}$ . (SFG spectra of deuterated hydrocarbon chains in the C–D region frequently show additional small resonances even in close packed monolayers.) Nevertheless the prominent  $r$  resonances observed in Figure 10 are consistent with close packing of the d-DPPE lipid chains leading to a highly ordered all-trans conformation. Since the resonances appear as peaks, it shows unambiguously that the d-methyl groups contributing to this spectrum are oriented into the bilayer, i.e. have the opposite orientation to that of the proximal leaflet.

For comparison, the PPP spectrum in the C–D region of a d-ODT self-assembled monolayer on gold in air, which is known to be close packed and therefore highly ordered, is shown in the middle spectrum in Figure 10. The difference in the positions of the  $r$  resonances between the d-DPPE and d-ODT spectra is due to the different media above the bilayers. It is well-known that SFG spectra recorded in air lie at a slightly lower frequency ( $\sim 5\text{--}10\text{ cm}^{-1}$ ) than those recorded under water. The PPP spectrum in the C–H region of the bilayer using a DPPE distal leaflet formed by LB deposition on a d-DPPE/activated d-MUA SAM is shown in Figure 10 (bottom spectrum). As in Figure 10 (top spectrum) the three  $r$  resonances are very prominent features, indicating a highly ordered and close-packed distal monolayer.

In order to employ SFG spectroscopy to investigate the behavior of the distal and proximal leaflets of bilayer membranes separately when they are exposed to membrane proteins and other membrane-sensitive molecules, the leaflets are required to be isotopically distinguishable. The method of vesicle fusion commonly used to form bilayers generates the distal and proximal leaflets simultaneously and therefore cannot be used to generate a bilayer composed of isotopically different leaflets. The current experiments provide an assessment of the integrity of isotopically asymmetric bilayers when only the distal leaflet is formed by vesicle fusion onto a preformed proximal leaflet. The d-DPPE and DPPE SFG spectra of the distal leaflets presented in Figures 9 and 10 provide strong spectral evidence that a distal leaflet formed by LB deposition is of higher quality, in terms of both packing density and conformational order, than a distal leaflet formed using vesicle fusion. This suggests that over short time scales at least the LB method provides a procedure for forming conformationally well-ordered distal leaflets that is more reliable than that from vesicle fusion. Furthermore, by comparing the distal leaflet formed by LB deposition with the proximal leaflet formed by self-assembly on an activated SAM (Figure 5), it can be seen

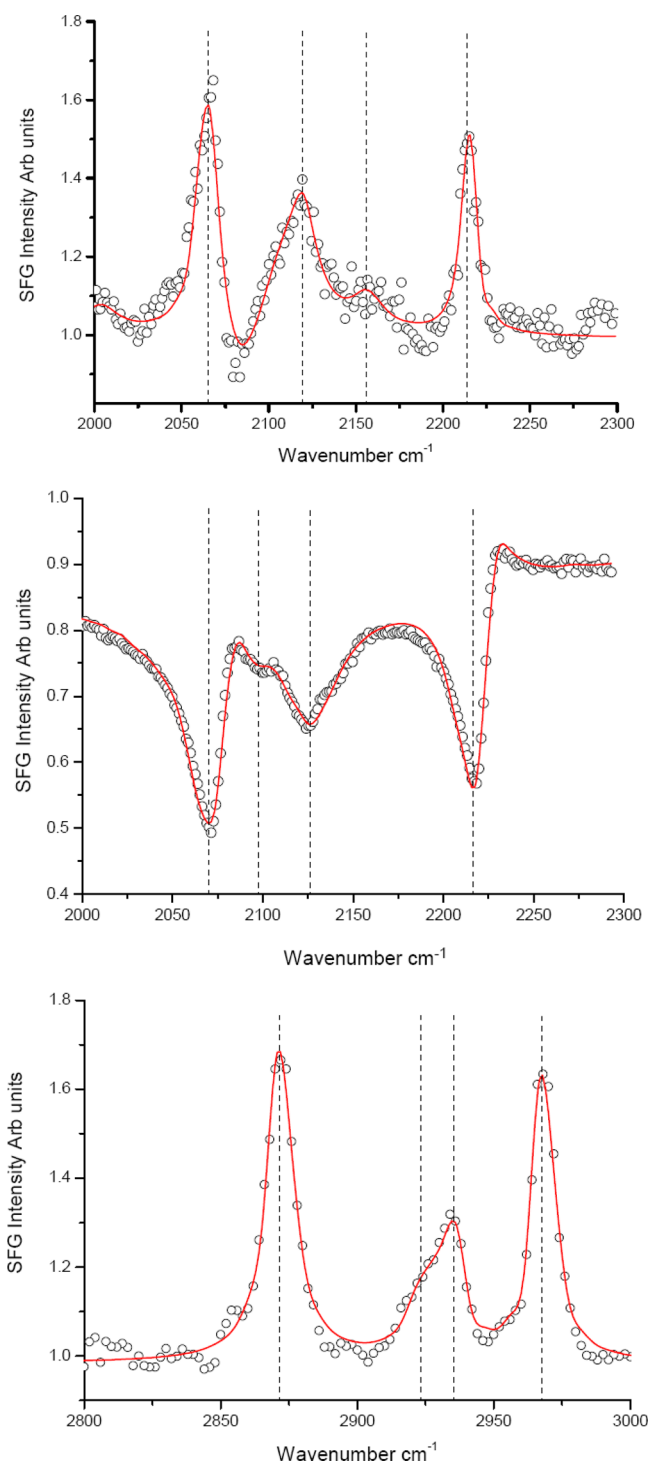


**Figure 10.** SFG spectra in the PPP polarization combination. Top spectrum: bilayer consisting of a d-DPPE distal leaflet LB cast onto a DPPE proximal leaflet bound to an activated MUA SAM recorded in the C–D region. Middle spectrum: d-ODT SAM on gold under air recorded in the C–D region. Bottom spectrum: bilayer consisting of a DPPE distal leaflet LB cast onto a d-DPPE proximal leaflet bound to an activated d-MUA SAM recorded in the C–H region.

that the distal leaflet is more ordered with essentially a complete absence of  $d$  resonances arising from gauche defects. Finally, the spectra in Figure 5 show that the proximal leaflet formed by LB deposition is only marginally better ordered than that formed by self-assembly. It is interesting to note that the

commonly used procedure for binding homogeneous bilayers to activated MUA by VF is the same as one of the methods used here to attach the proximal leaflet, namely self-assembly leading to the formation of an amide bond. This suggests that the proximal leaflet of a homogeneous bilayer formed by vesicle fusion to a hydrophilic activated MUA SAM may be of conformational order similar to that found for the proximal leaflet formed by LB deposition in this study.

## CONCLUSION

In this work SFG vibrational spectroscopy, supported by RAIRS, has been used to provide detailed structural insight into the stepwise construction of SBMs of lipid bilayers formed on MUA SAMs. By using MUA SAMs and lipid layers that were per-protonated or per-deuterated it was possible to examine the orientation and conformation of each of the components, namely distal lipid leaflet, proximal lipid leaflet, and MUA/gold SAM, as they were bound stepwise to the MUA monolayer. Prior to forming lipid bilayers the MUA or d-MUA SAM was activated using the established EDC/NHS procedure to form a succinimide ester top layer. This was confirmed from the changes in the RAIRS and SFG spectra following activation. A per-protonated or per-deuterated DPPE proximal leaflet was then bound to the activated SAM by an amide bond following self-assembly or LB adsorption. The conformational ordering of the MUA SAM on the gold substrate is significantly improved after the adsorption of the DPPE proximal leaflet to the activated SAM. SFG spectroscopy of this layer showed that it was quite well ordered but still showed evidence of gauche defects in the lipid hydrocarbon chains. There was little difference in the films formed by self-assembly or LB methods, indicating that the packing density in this leaflet is most likely controlled by the formation of the amide bond. The distal leaflet was formed either by LB or VF deposition. The distal leaflet formed on the activated MUA/proximal leaflet by vesicle fusion shows significantly lower conformational ordering than that formed by LB deposition. The latter was highly ordered with little evidence of gauche defects in the SFG spectra. Furthermore the DPPE chains were more ordered than in the proximal leaflet of the bilayer. It is therefore concluded that LB deposition is the preferred method for the construction of isotopically asymmetric supported lipid bilayers on activated hydrophilic self-assembled monolayers on gold. As well as confirming the formation of a SBM using SFG spectroscopy, the polar orientation of all the layers has been unambiguously deduced from the phase of the SFG spectra. This SAM/lipid system is stable under water.

## ASSOCIATED CONTENT

### Supporting Information

Additional spectra comprising the SSP spectra of MUA, a comparison of the pico- and femtosecond spectra of MUA and the SFG spectra recorded at the air/liquid interface of the MUA melt; SFG fitting procedure. This material is available free of charge via the Internet at <http://pubs.acs.org>.

## AUTHOR INFORMATION

### Corresponding Authors

\* E-mail: [ye@cat.hokudai.ac.jp](mailto:ye@cat.hokudai.ac.jp). Telephone: +81 117 069126 (S.Y.).

\* E-mail: [pbd2@cam.ac.uk](mailto:pbd2@cam.ac.uk). Telephone: +44 1223 336460 (P.B.D.).

## Notes

The authors declare no competing financial interest.

## ACKNOWLEDGMENTS

M.T.L.C. acknowledges the Japan Society for the Promotion of Science (JSPS) for the award of a Fellowship for Research in Japan (PE 11042). S.Y. acknowledges a Grant-in-Aid for Scientific Research (B) 23350058 and a Grant-in-Aid for Scientific Research on Innovative Areas "Coordination program" (24108701) from MEXT, Japan.

## REFERENCES

- (1) Tamm, L. K.; McConnell, H. M. Supported phospholipid bilayers. *Biophys. J.* **1985**, *47* (1), 105–113.
- (2) Tamm, L. K. Lateral diffusion and fluorescence microscope studies on a monoclonal-antibody specifically bound to supported phospholipid-bilayers. *Biochemistry* **1988**, *27* (5), 1450–1457.
- (3) Meuse, C. W.; Krueger, S.; Majkrzak, C. F.; Dura, J. A.; Fu, J.; Connor, J. T.; Plant, A. L. Hybrid bilayer membranes in air and water: Infrared spectroscopy and neutron reflectivity studies. *Biophys. J.* **1998**, *74* (3), 1388–1398.
- (4) Meuse, C. W.; Niaura, G.; Lewis, M. L.; Plant, A. L. Assessing the molecular structure of alkanethiol monolayers in hybrid bilayer membranes with vibrational spectroscopies. *Langmuir* **1998**, *14* (7), 1604–1611.
- (5) Lahiri, J.; Isaacs, L.; Tien, J.; Whitesides, G. M. A strategy for the generation of surfaces presenting ligands for studies of binding based on an active ester as a common reactive intermediate: A surface plasmon resonance study. *Anal. Chem.* **1999**, *71* (4), 777–790.
- (6) Fischer, T.; Senin, I. I.; Philipopov, P. P.; Kock, K.-W. Application of different lipid surfaces to monitor protein–membrane interactions by surface plasmon resonance spectroscopy. *Spectroscopy* **2002**, *16*, 271–279.
- (7) Sam, S.; Touahir, L.; Andresa, J. S.; Allongue, P.; Chazalviel, J. N.; Gouget-Laemmel, A. C.; de Villeneuve, C. H.; Moraillon, A.; Ozanam, F.; Gabouze, N.; et al. Semiquantitative study of the EDC/NHS activation of acid terminal groups at modified porous silicon surfaces. *Langmuir* **2010**, *26* (2), 809–814.
- (8) Touahir, L.; Chazalviel, J. N.; Sam, S.; Moraillon, A.; de Villeneuve, C. H.; Allongue, P.; Ozanam, F.; Gouget-Laemmel, A. C. Kinetics of activation of carboxyls to succinimidyl ester groups in monolayers grafted on silicon: An in situ real-time infrared spectroscopy study. *J. Phys. Chem. C* **2011**, *115* (14), 6782–6787.
- (9) Brian, A. A.; McConnell, H. M. Allogenic stimulation of cytotoxic T cells by supported planar membranes. *Proc. Natl. Acad. Sci. U.S.A.* **1984**, *81*, 6159–6163.
- (10) Ulman, A. *An Introduction to Ultrathin Films: From Langmuir-Blodgett to Self Assembly*, 1st ed.; Academic Press Ltd.: London, 1991.
- (11) Lipkowski, J. Building biomimetic membrane at a gold electrode surface. *Phys. Chem. Chem. Phys.* **2010**, *12* (42), 13874–13887.
- (12) Li, M.; Chen, M.; Sheepwash, E.; Brosseau, C. L.; Li, H.; Pettinger, B.; Gruler, H.; Lipkowski, J. AFM studies of solid-supported lipid bilayers formed at a Au(111) electrode surface using vesicle fusion and a combination of Langmuir–Blodgett and Langmuir–Schaefer techniques. *Langmuir* **2008**, *24* (18), 10313–10323.
- (13) Woodward, J. T.; Meuse, C. W. Mechanism of formation of vesicle fused phospholipid monolayers on alkanethiol self-assembled monolayer supports. *J. Colloid Interface Sci.* **2009**, *334* (2), 139–145.
- (14) Venkatesan, B. M.; Polans, J.; Comer, J.; Sridhar, S.; Wendell, D.; Aksimentiev, A.; Bashir, R. Lipid bilayer coated  $\text{Al}_2\text{O}_3$  nanopore sensors: towards a hybrid biological solid-state nanopore. *Biomed. Microdevices* **2011**, *13* (4), 671–682.
- (15) Richter, R.; Mukhopadhyay, A.; Brisson, A. Pathways of lipid vesicle deposition on solid surfaces: A combined QCM-D and AFM study. *Biophys. J.* **2003**, *85* (5), 3035–3047.
- (16) Tawa, K.; Morigaki, K. Substrate-supported phospholipid membranes studied by surface plasmon resonance and surface

plasmon fluorescence spectroscopy. *Biophys. J.* **2005**, *89* (4), 2750–2758.

(17) Tatulian, S. A. Attenuated total reflection Fourier transform infrared spectroscopy: A method of choice for studying membrane proteins and lipids. *Biochemistry* **2003**, *42* (41), 11898–11907.

(18) Bain, C. D. Sum-frequency vibrational spectroscopy of the solid-liquid interface. *J. Chem. Soc., Faraday Trans.* **1995**, *91* (9), 1281–1296.

(19) Lambert, A. G.; Davies, P. B.; Neivandt, D. J. Implementing the theory of sum frequency generation vibrational spectroscopy: A tutorial review. *Appl. Spectrosc. Rev.* **2005**, *40*, 103–145.

(20) Shen, Y. R. *The Principles of Non-Linear Optics*; Wiley: New York, 1984.

(21) Kett, P. J. N.; Casford, M. T. L.; Davies, P. B. Structure of mixed phosphatidylethanolamine and cholesterol monolayers in a supported hybrid bilayer membrane studied by sum frequency generation vibrational spectroscopy. *J. Phys. Chem. B* **2011**, *115* (20), 6465–6473.

(22) Press, W. H.; Fannery, B. P.; Taukolsky, S. A.; Vetterling, W. T. *Numerical Recipes*; Cambridge University Press: Cambridge, 1989.

(23) Ye, S.; Noda, H.; Nishida, T.; Morita, S.; Osawa, M. Cd<sup>2+</sup>-induced interfacial structural changes of Langmuir–Blodgett films of stearic acid on solid substrates: A sum frequency generation study. *Langmuir* **2004**, *20* (2), 357–365.

(24) Wang, J.; Chen, C. Y.; Buck, S. M.; Chen, Z. Molecular chemical structure on poly(methyl methacrylate)(PMMA) surface studied by sum frequency generation (SFG) vibrational spectroscopy. *J. Phys. Chem. B* **2001**, *105* (48), 12118–12125.

(25) Asanuma, H.; Noguchi, H.; Uosaki, K.; Yu, H. Z. Structure and reactivity of alkoxycarbonyl(ester)-terminated monolayers on silicon: Sum frequency generation spectroscopy. *J. Phys. Chem. B* **2006**, *110* (10), 4892–4899.

(26) Lu, R.; Gan, W.; Wu, B. H.; Chen, H.; Wang, H. F. Vibrational polarization spectroscopy of CH stretching modes of the methylene group at the vapor/liquid interfaces with sum frequency generation. *J. Phys. Chem. B* **2004**, *108* (22), 7297–7306.

(27) Stamboliyska, B. A.; Binev, Y. I.; Radomirska, V. B.; Tsenov, J. A.; Juchnovski, I. N. IR spectra and structure of 2,5-pyrrolidinedione-(succinimide) and of its nitranion: experimental and ab initio MO studies. *J. Mol. Struct.* **2000**, *516* (2–3), 237–245.

(28) Woldbaek, T.; Klæboe, P.; Christensen, D. H. Vibrational spectra of succinimide and *N*-deuteriosuccinimide. *Acta Chem. Scand. Ser. A* **1976**, *30* (7), 531–539.

(29) Kett, P. J. N.; Casford, M. T. L.; Yang, A. Y.; Lane, T. J.; Johal, M. S.; Davies, P. B. Structural changes in a polyelectrolyte multilayer assembly investigated by reflection absorption infrared spectroscopy and sum frequency generation spectroscopy. *J. Phys. Chem. B* **2009**, *113* (6), 1559–1568.

(30) Xiao, S. J.; Brunner, S.; Wieland, M. Reactions of surface amines with heterobifunctional cross-linkers bearing both succinimidyl ester and maleimide for grafting biomolecules. *J. Phys. Chem. B* **2004**, *108* (42), 16508–16517.

(31) Sunder, S.; Cameron, D. G.; Casal, H. L.; Boulanger, Y.; Mantsch, H. H. Infrared and Raman-spectra of specifically deuterated 1,2-dipalmitoyl-*sn*-glycero-3-phosphocholines. *Chem. Phys. Lipids* **1981**, *28* (2), 137–147.

(32) le Maire, M.; Champeil, P.; Møller, J. V. Interaction of membrane proteins and lipids with solubilizing detergents. *Biochim. Biophys. Acta: Biomembr.* **2000**, *1508* (1–2), 86–111.